HARVARD SEMITIC MUSEUM PUBLICATIONS

Lawrence E. Stager, General Editor
Michael D. Coogan, Director of Publications

FINAL REPORTS OF THE LEON LEVY EXPEDITION TO ASHKELON

Series Editors
Lawrence E. Stager, Daniel M. Master, and J. David Schloen

1. *Ashkelon 1: Introduction and Overview (1985–2006)*
   edited by Lawrence E. Stager, J. David Schloen, and Daniel M. Master
2. *Ashkelon 2: Imported Pottery of the Roman and Late Roman Periods*
   by Barbara L. Johnson
3. *Ashkelon 3: The Seventh Century B.C.*
   by Lawrence E. Stager, Daniel M. Master, and J. David Schloen
4. *Ashkelon 4: The Iron Age Figurines of Ashkelon and Philistia*
   by Michael D. Press
5. *Ashkelon 5: The Land behind Ashkelon*
   by Yaakov Huster
6. *Ashkelon 6: The Middle Bronze Age Ramparts and Gates of the North Slope and Later Fortifications*
   Edited by Lawrence E. Stager, J. David Schloen, and Ross J. Voss
7. *Ashkelon 7: The Iron Age I*
   Edited by Lawrence E. Stager, Daniel M. Master, and Adam J. Aja
8. *Ashkelon 8: The Islamic and Crusader Periods*
   by Tracy Hoffman

THE LEON LEVY EXPEDITION TO ASHKELON

ASHKELON 8

The Islamic and Crusader Periods

by

Tracy Hoffman

With contributions by

Denys Pringle, Hannah Buckingham, Frances Healy, Tasha Vorderstrasse, Christopher Bronk Ramsey, Robert Kool, Robyn Le Blanc, Kathleen M. Forste, John M. Marston, Paula Hesse, and Deirdre N. Fulton

University Park, Pennsylvania
EISENBRAUNS
2019

Ashkelon 8:
The Islamic and Crusader Periods

by Tracy Hoffman

with contributions by

Denys Pringle, Hannah Buckingham, Frances Healy, Tasha Vorderstrasse, Christopher Bronk Ramsey, Robert Kool, Robyn Le Blanc, Kathleen M. Forste, John M. Marston, Paula Hesse, and Deirdre N. Fulton

Printed in the U.S.A.

Distributed by
Eisenbrauns
an imprint of Penn State University Press
University Park, Pennsylvania

http://eisenbrauns.org

Library of Congress Cataloging-in-Publication Data

The paper used in this publication meets the minimum requirements of the American National Standard for Information Sciences—Permanence of Paper for Printed Library Materials, ANSI Z39.48–1984. ♾™

TABLE OF CONTENTS

Abbreviations ix
Contributors xi
Editors' Preface xiii
Author's Preface xv

PART ONE:
HISTORICAL SETTING, ARCHITECTURE, AND STRATIGRAPHY

1. Introduction 3

THE NORTH TELL

2. Grid 9 Workshop 13
3. Grid 16 Residential Quarter 16
4. Grid 23 Residential Quarter 19
5. Grid 2 British Mandate Road 24

THE SOUTH TELL

6. Grid 25 Mixed-Use Building 25
7. Grid 32 Residential Courtyard 30
8. Grid 34/41 Church 33
9. Grid 37 House 39
10. Grid 38 Residential Quarter 45
11. Grid 44 Mixed-Use Residential Quarter 49
12. Grid 47 Residential Quarter 57
13. Grid 50 and 51 Pits and Robber Trenches 66
14. Grid 57 Mixed-Use Residential Quarter 69
15. Grid 64 Residential Courtyard 71

THE FORTIFICATIONS

16. Grid 3/10 Fortifications 73
17. Grid 20 Fortification Tower *Hannah Buckingham and Denys Pringle* 76
18. Grid 35 Jerusalem Gate 91

PART TWO:
THE WALLS OF ASHKELON

19. The Survey of the Walls of Ashkelon *Denys Pringle* 97
20. The Radiocarbon Dating of the Walls of Ashkelon *Denys Pringle, Frances Healy, and Christopher Bronk Ramsey* 222

PART THREE:
POTTERY

21. Ceramic Corpus 247
22. Lamps 465
23. Chinese Ceramics *Tasha Vorderstrasse* 506

PART FOUR:
OTHER ARTIFACTS

24. Coins *Robert Kool* 523
25. Glass *Robyn Le Blanc* 575
26. Metals *Hannah Buckingham* 629

PART FIVE:
ORGANIC REMAINS

27. Plant Remains *Kathleen M. Forste and John M. Marston* 645
28. Animal Remains from Fatimid and Crusader Ashkelon *Paula Hesse and Deirdre N. Fulton* 666

PART SIX:
CONCLUSIONS

29. Conclusion 701

Bibliography 711

Concordance Of Stratigraphic Contexts 747

Index. 771

20. The Radiocarbon Dating of the Walls of Ashkelon

by Denys Pringle, Frances Healy, and Christopher Bronk Ramsey

The program of radiocarbon dating reported on here sprang from Denys Pringle's detailed survey and analysis of the surviving fragments of Ashkelon's Byzantine and medieval town walls (see Chapter 19, this volume). It aimed to enhance the chronological precision of the structural sequence already constructed on the basis of the characterization of different masonry and mortar types within individual wall fragments and to test the proposed dates of specific masonry contexts by obtaining radiocarbon dates from them and modeling them within a Bayesian framework.

Practical Considerations

Much of the mortar used in constructing the walls of Ashkelon clearly contains charcoal and other charred plant remains, which were apparently derived from the fuel burnt when slaking the lime used in building them. Indeed, in the 1970s, a charcoal sample taken from the wall near the Jerusalem Gate had been dated to the Byzantine period (Kedar and Mook 1978). This appeared to suggest a straightforward way of dating further wall fragments, always assuming that the charcoal was contemporary with the mortar.

An alternative would have been to date the mortars themselves. The essentials of the method and its principal problems have long been established, the main hurdle being the elimination from the samples of carbonates other than ^{14}C from CO_2 absorbed from the atmosphere during hardening. The principal potential sources of contamination are: (1) natural carbonates of geological age, totally depleted in ^{14}C, derived either from incompletely slaked limestone or from sand or aggregate added to the mortar; and (2) the ability of mortar, once it has set, to absorb additional carbon from carbonates dissolved in rain or groundwater, which may reflect the levels of atmospheric ^{14}C of periods earlier or later than the time when the mortar was mixed (van Strydonk et al. 1986). Much methodological progress has been made here, both in pretreatment and in radiocarbon age calculation (e.g., Nonni et al. 2013; Ringbom et al. 2014), methods of pretreatment varying with mortar type. The processes, however, remain more complex and more experimental than those employed for dating charcoal. This aside, at Ashkelon, dating the mortar itself would have met with two particular problems. The marine shell present in varying quantities in many of the mortars would, if not all marine carbons were removed in pretreatment, have carried a risk of producing results that were too old, since the surface marine environment is diluted by the upwelling of radiocarbon-depleted water from the deep oceans. Furthermore, all the samples except those from the excavation of the wall FF (phase 6) in Grid 20 were collected from upstanding fragments of wall that had been exposed to the elements for centuries, thus risking the uptake of carbon from rainwater (mortar samples from exposed walls are ideally drilled from deep within them). There was thus a persuasive case for attempting to date the walls with charcoal samples rather than mortar ones.

We therefore set out to obtain three short-life samples of charcoal or charred plant material from each selected building context. Dating single fragments would eliminate the risk of combining material of different ages in the same sample (Ashmore 1999); and, even if all three resulting measurements were not statistically consistent, the most recent would probably be close in age to the date of construction. In practice, however, obtaining three suitable samples from each context proved to be more difficult than anticipated.

Out of 69 different building contexts identified at 36 different locations (see Chapter 19, this volume, table 19.3), samples were retrieved from only 43 building contexts (29 locations); and out of these, only 15 building contexts (13 locations) gave at least one radiocarbon date. This shortfall was due in the first place to the general lack of carbonized material from some masonry contexts (usually those dating from the Fatimid period onward), and secondly to the unsuitability of some of the samples collected, which proved to be too small for identification, or not to be charcoal or charred plant remains at all. A third winnowing of the number of samples occurred as a result of 17 of the 59 samples submitted for dating producing insufficient yields, leaving us with a total of 42 dates from 15 contexts at 13 locations. Nevertheless, these contexts ranged around all parts of the surviving walls and covered all the main building periods previously identified.

The 15 building contexts provided between one and four dates each, counting replicate measurements on a single sample as one. Three samples were single-season growths in the form of seeds or leaves. Twenty were of twig charcoal, a few years old at most, regardless of taxon. Sixteen were from branches or logs, generally of fig, pine, or oak. Here there is a stronger possibility of age offsets, especially with oak, but also

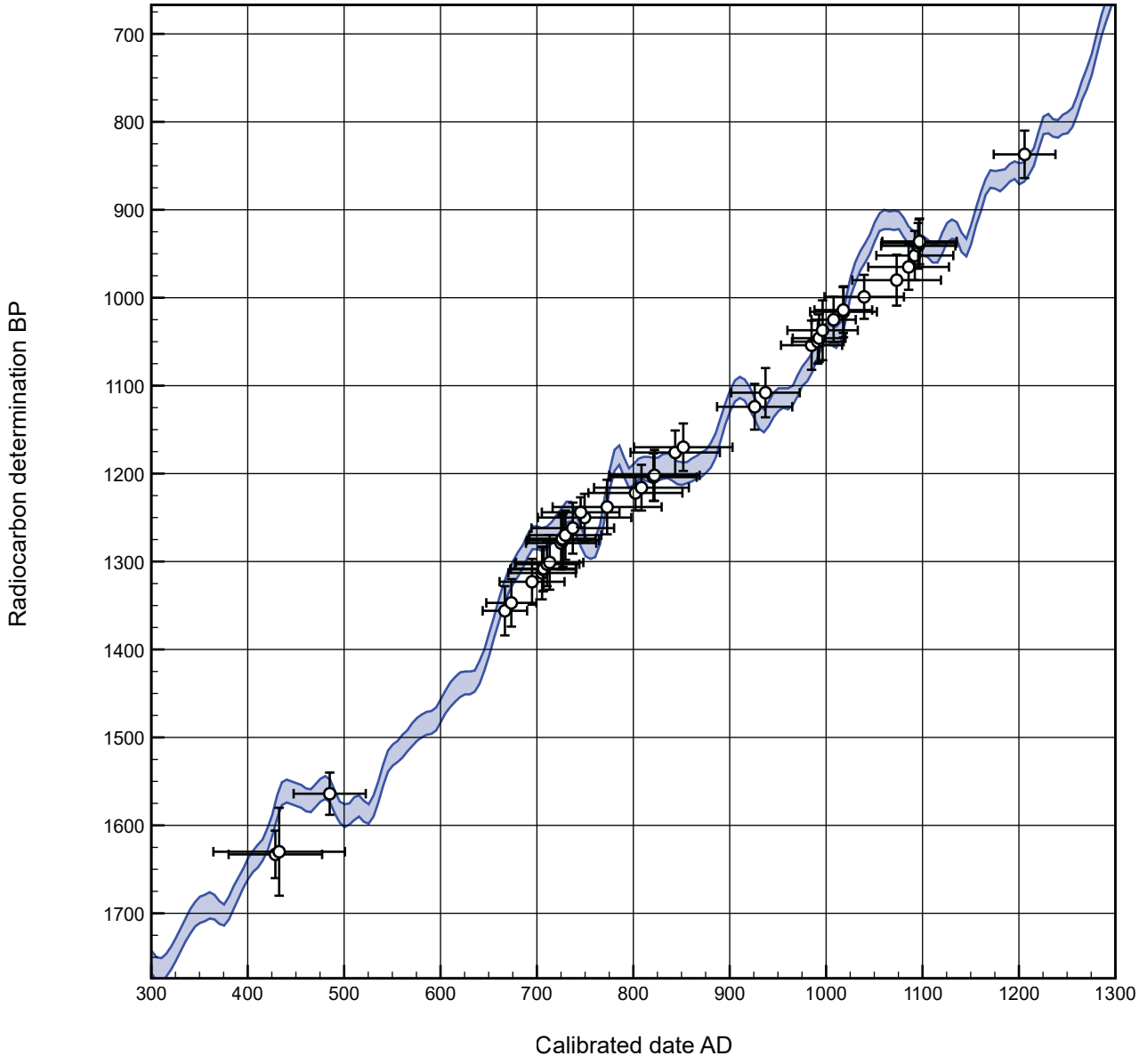

Figure 20.1. Radiocarbon determinations from the post-classical walls of Ashkelon, plotted against the IntCal13 calibration curve

with pine, some local varieties of which can live up to 150 years.[1] The fact that all the more mature fragments were from branches or logs, i.e., roundwood, however, reduces the likelihood that they would have been many decades old or that they could have represented reused timbers from ships or buildings, which could introduce further age offsets. Samples that could not be identified to species or genus were assigned to the broad divisions of gymnosperm (in this context conifers) or angiosperm (in this context deciduous trees).

The radiocarbon calibration curve for the period during which the walls were built includes plateaux, in the sense of wiggles, which make the distributions of calibrated date ranges longer than they otherwise would be, notably in the late seventh to mid-eighth and late eighth to mid-ninth centuries A.D., with a lesser one in the late eleventh to mid-twelfth century A.D. (figure 20.1).

[1] Information kindly provided by Dr. Stephen Harris.

Methods

Radiocarbon Dating

Dating was undertaken by the University of Oxford Radiocarbon Accelerator Unit. The samples underwent solvent extraction to remove contaminants such as traces of glue, prior to acid-base-acid treatment, gelatinization, and ultrafiltration (Brock et al. 2010:106–107: pretreatments AF, AF*). They were then combusted and graphitized as described by Brock et al. (2010:110) and Dee and Bronk Ramsey (2000), and dated by Accelerator Mass Spectrometry (AMS) (Bronk Ramsey et al. 2004). $\delta^{13}C$ values were measured independently by Isotope Ratio Mass Spectrometry (IRMS) as described by Brock et al. (2010:110). The laboratory maintains continuous programs of internal quality control and also takes part in international intercomparisons (Scott 2003; Scott et al. 2007; 2010a; 2010b).

Forty-four radiocarbon results were obtained, including two pairs of replicates (i.e., independent determinations on two parts of the same sample). The results are set out in table 20.1. All radiocarbon results are conventional radiocarbon ages, corrected for fractionation (Stuiver and Polach 1977).

Chronological Modeling

The principle behind the Bayesian approach to the interpretation of data is encapsulated by Bayes's theorem (Bayes 1763). In essence, new data collected about a problem ("the standardized likelihoods") are analyzed in the context of existing experience and knowledge of that problem ("prior beliefs"). The combination of the two permits a new understanding of the problem ("posterior beliefs"), which can in turn become prior beliefs in a subsequent model. Bayesian analysis can be used to bring together archaeological information and radiocarbon information by expressing both as probability density functions, which are also the form of the posterior beliefs. In the modeling of archaeological chronologies, calibrated radiocarbon dates form the "standardized likelihoods" component of the model, and archaeology provides the "prior beliefs." The radiocarbon dates are thus reinterpreted in the light of the archaeological information to provide posterior beliefs about the dates. The resulting estimates will vary with the model(s) employed, and several different models may be constructed based on varying interpretations of the same data (Bayliss et al. 2007). The purpose of modeling is to progress beyond the date at which individual samples left the carbon cycle to the dates of the archaeological events associated with those samples.

The chronological modeling has been undertaken using OxCal 4.2.4 (Bronk Ramsey 1995; 1998; 2009; Bronk Ramsey et al. 2010; Bronk Ramsey and Lee 2013), and the internationally agreed calibration curve for terrestrial samples from the northern hemisphere (IntCal13; Reimer et al. 2013). Calibrations have been calculated using the probability method (Stuiver and Reimer 1993). Once the probability distributions of individual calibrated results have been calculated, the program attempts to reconcile these distributions with the prior information by repeatedly sampling each distribution to build up a set of solutions consistent with the model structure. This is done using a random sampling technique, Markov Chain Monte Carlo (MCMC), which generates a representative set of possible combinations of dates. This process produces a posterior probability distribution for each sample's calendar age, which occupies only a part of the calibrated probability distribution. Posterior probability distributions are cited *in italics* to distinguish them from simple calibrated date ranges and are rounded outward to the nearest five years. In figures 20.3–4 the posterior density estimates are shown in solid black and the calibrated radiocarbon dates from which they have been sampled are shown in outline. In the case of OxA-30949, for example, a simple calibration of cal A.D. 670–890 (2σ) is reduced to a Highest Posterior Density Interval of *cal A.D. 675–830* (*95% probability*; figure 20.3). Some posterior density estimates do not directly map particular radiocarbon dates, although they are calculated from them. These include estimates of the dates of particular events (e.g., figure 20.3: *build VV*), the durations of episodes, and the intervals between events.

Statistics calculated by OxCal provide guides to the reliability of a model. One is the individual index of agreement, which expresses the consistency of the prior and posterior distributions. If the posterior distribution is situated in a high-probability region of the prior distribution, the index of agreement is high (sometimes 100 or more, e.g., figure 20.3: *OxA-30949* [A: 114]). If the index of agreement falls below 60 (a threshold value analogous to the 95% significance level in a χ^2 test), the radiocarbon date is regarded as inconsistent with the sample's calendar age. Sometimes this merely indicates that the radiocarbon result is a statistical outlier (more than two standard deviations from the sample's true radiocarbon age), but a very low index of agreement may mean that the sample is redeposited or intrusive (i.e., that its calendar age is different from that implied by its context), or that it is contaminated with extraneous carbon. Another index of agreement, Amodel, is calculated from the individual agreement indices and indicates whether the model

Table 20.1: Radiocarbon Dates. The calibrations in the 'Calibrated date range 2σ' column are calculated by the maximum intercept method (Stuiver and Reimer 1986) and are cited as recommended by Mook (1986): rounded outward by 10 if the standard deviation is 25 or more, by 5 if it is less than 25. Those in the 'Highest Posterior Density Interval cal BC' column are rounded outward by 5 and are derived from model 1 (Figs 2–5). All samples were of charcoal or charred plant remains.

Frag. (phase)	*Grid*	*Context*	*Sample no.*	*Laboratory no.*	*BP*	*δ13CIRMS ‰*	*Weighted mean BP*	*Calibrated AD 2σ*	*Highest Posterior Density Interval cal AD (95% probability)*	*Identification*
B (1)	64	Sea wall	8	OxA-failed	-	-	-	-	-	Angiosperm. Twigs.
B (2)	64	Sea wall: possibly from an earlier building	9	OxA-30713	1564±24	−24.2±0.3	-	415–565	*420–550*	Large branch, probably *Ficus*
BB2	35	Intermediate gate	69	OxA-failed	-	-	-	-	-	Twig. Gymnosperm.
C (2)	72	Land wall	10	OxA-30714	1258±24	−27.3±0.3	1244±17 T'=0.7; T'(5%)=3.8; ν=1	685–800	*680–780* (93%) *790–805* (2%)	Large branch, probably *Quercus*. Replicate of OxA-30715
C (2)	72	Land wall	10	OxA-30715	1230±24	−26.4±0.3				Replicate of OxA-30714
C (2)	72	Land wall	11	OxA-failed	-	-	-	-	-	Large branch, appears to have been waterlogged or only partially carbonised. Probably gymnosperm.
C (2)	72	Land wall	12	OxA-30945	1276±30	−26.0±0.3	-	660–780	*670–775*	Large branch, probably *Ficus*. Appears to have been waterlogged or only partially carbonised.
D	75	Tower: SW corner	91	OxA-30643	837±27	−23.6±0.3	-	1150–1270	*1055–1065* (1%) *1155–1265* (94%)	Branch/log at least five years old. *Pinus*.
D	75	Tower: E fracture	93	OxA-30556	1016±29	−24.7±0.3	-	980–1040	*975–1045* (82%) *1090–1125* (10%) *1135–1150* (3%)	Twig. Probably gymnosperm.
E (2)	69	Land wall	16	OxA-failed	-	-	-	-	-	Twig, probably *Ficus*.
E (2)	69	Land wall	17	OxA-failed	-	-	-	-		Large branch, probably gymnosperm
F1 (1)	62	Feature attached to wall	19	OxA-failed	-	-	-	-	-	Probably gymnosperm. Appears to have been waterlogged or only partially carbonised.
F1 (1)	62	Feature attached to wall	20	OxA-30919	938±27	−21.5±0.3	-	1020–1170	*1025–1160*	*Olea europaea* endocarp
F1 (2)	62	Land Wall	22	OxA-failed	-	-	-	-	-	Twig. Probably angiosperm.

FF (6)	20	Wall 26	207	OxA-failed	-	-	-	-	-	Appears to be angiosperm wood.
FF (6)	20	Wall 26	208	OxA-failed	-	-	-	-	-	Remains of carbonised fruit/ seed, probably *Olea europaea* endocarp.
FF (6)	20	Wall 28	212	OxA-failed	-	-	-	-	-	Carbonised *Olea europaea* endocarp.
FF (6)	20	Wall 90	219	OxA-33101	1046±27	−21.1±0.3	-	900–1030	*900–920* (3%) *960–1025* (92%)	Carbonised fruit/seed remains, probably Poaceae.
FF (6)	20	Walll 90	221	OxA-33102	1108±28	−25.1±0.3	-	880–1000	*900–1015*	Appears to be layers of carbonized leaves (possibly Arecaceae) mixed with some wood charcoal.
FF (6)	20	Wall 90	222	OxA-33103	1037±34	−22.2±0.3	-	900–1040	*900–920* (3%) *950–1030* (92%)	Charcoal fragment; appears to be one-year-old angiosperm twig.
H (1)	49	Tower added to wall	33	OxA-failed	-	-	-	-	-	Twig. Probably *Ficus*
H (1)	49	Tower added to wall	35	OxA-failed	-	-	-	-	-	Twig. Probably gymnosperm.
H (2)	49	Land wall	30	OxA-30920	1262±29	−22.9±0.3	-	660–860	*670–780* (81%) *790–865* (14%)	Large branch/log at least 7 years old. *Pinus*.
H (2)	49	Land wall	32	OxA-30921	1202±29	−23.4±0.3	-	710–940	*705–745* (13%) *765–890* (82%)	Large branch/log at least 4 years old. *Pinus*.
JJ3 (1)	78	Land wall	13	OxA-31025	941±26	−24.5±0.3	-	1020–1170	*1030–1155*	Branch at least 9 years old, probably *Pinus*.
JJ3 (1)	78	Land wall	15	OxA-31024	936±26	−26.0±0.3	-	1020–1170	*1030–1155*	Branch, at least 5 years old, probably *Quercus*.
K (1)	41	Rounded tower: concentration of charcoal between two courses	49	OxA-30969	1054±28	−25.6±0.3	1003±20 T'=6.6; T'(5%)=3.8; ν=1	900–1030	*985–1045*	Twig, internal preservation too poor for ID. Different fragment from that dated by OxA-30970
K (1)	41	Rounded Tower: concentration of charcoal between two courses	49	OxA-30970	952±28	−27.0±0.3		1020–1160		As OxA-30969, different fragment from that dated by OxA-30969
K (1)	41	Rounded tower	223	OxA-32877	1014±26	−23.3±0.3	-	990–1040	*975–1045*	Charcoal fragment; angiosperm twig at least two years old but given diameter not more than four years old.

K (1)	41	Rounded tower	224	OxA-32878	999±25	−23.4±0.3	-	1000–1110	*985–1050* (88%) *1090–1120* (7%)	Charcoal fragment; three-year-old twig, probably *Olea europaea*
K (1)	41	Rounded tower	225	OxA-32879	965±26	−23.3±0.3	-	1020–1150	*1015–1130* (91%) *1135–1150* (4%)	Charcoal fragment; one-year-old *Quercus* twig.
K (2)	41	Rebuilding land wall	44	OxA-30946	1313±30	−25.9±0.3	-	650–770	*655–725* (69%) *735–770* (26%)	Twig, 1 year old. Angiosperm.
K (2)	41	Rebuilding land wall	45	OxA-30947	1301±31	−21.1±0.3	-	650–780	*660–730* (64%) *735–770* (31%)	Branch/ large log. *Pinus*
K (2)	41	Rebuilding land wall	46	OxA-30922	1356±28	−22.1±0.3	-	640–690	*635–695* (90%) *700–710* (1%) *745–765* (4%)	Branch/ large log. *Pinus*
K (2)	41	Rebuilding land wall	47	OxA-31177	1347±27	−26.2±0.3	-	640–690	*640–695* (87%) *700–710* (2%) *745–765* (6%)	Twig at least 3 years old. *Pinus*.
K (3)	41	Land wall	40	OxA-failed	-	-	-	-	-	Twig. Probably gymnosperm. Appears to have been waterlogged or only partially carbonised.
K (3)	41	Land wall	42	OxA-failed	-	-	-	-	-	Twig. Probably gymnosperm. Appears to have been waterlogged or only partially carbonised.
N	1	Land wall	111	OxA-28792	1176±25	−24.4±0.3	-	770–950	*770–890*	Branch at least 4 years old, probably more. Probably *Ficus*.
N	1	Land wall	113	OxA-28793	1216±26	−25.3±0.3	-	690–890	*725–740* (2%) *765–885* (93%)	Branch at least 3 years old. Probably *Ficus*.
N	11	Land wall	114	OxA-28794	1181±28	−25.6±0.3	1222±20 T'=4.0; T'(5%)=3.8; ν=1	710–885	*725–740* (3%) *765–885* (92%)	Twig, 1 year old. Probably gymnosperm. Replicate of OxA-28785
N	11	Land wall	114	OxA-28795	1257±26	−25.6±0.3				Replicate of OxA-28784
R	11	Jaffa Gate: tower frag R1	105	OxA-28840	1025±26	−27.0±0.3	-	980–1040	*975–1035*	Twig, 1 year old. Probably *Ficus*.
R	11	Jaffa Gate: tower frag R1	106	OxA-28796	1124±26	−24.1±0.3	-	870–990	*890–995* (92%) *1000–1015* (3%)	Branch at least 4 years old. Probably *Ficus*

R	11	Jaffa Gate: tower frag R2	104	OxA-28839	1050±25	−24.4±0.3	-	900–1030	*960–1025*	Twig. Probably *Pinus*.
R	11	Jaffa Gate: tower frag R3	102	OxA-30948	980±29	−23.5±0.3	-	990–1160	*985–1060* (86%) *1080–1125* (9%)	Branch. Probably gymnosperm.
S	2	Land wall	108	OxA-31028	1204±27	−27.1±0.3	-	710–900	*725–740* (2%) *765–890* (93%)	Twig at least 2 years old. *Pinus*.
S	2	Land wall	109	OxA-31027	1250±27	−23.0±0.3	-	670–880	*690–780* (51%) *785–880* (44%)	Twig. *Pinus*.
S	2	Land wall	110	OxA-31026	1170±27	−26.3±0.3	-	770–970	*770–900* (94%) *925–940* (1%)	Branch/log at least 3 years old, probably more. *Pinus*.
VV	34	Triangular turret	53	OxA-30949	1238±31	−25.6±0.3	-	670–890	*675–830*	Twig, 1 year old. Internal preservation too poor for ID.
VV	34	Triangular turret	55	OxA-31030	1274±27	−22.9±0.3	-	660–780	*675–775*	Branch. Gymnosperm.
VV	34	Triangular turret	56	OxA-31029	1270±28	−26.5±0.3	-	660–780	*675–775*	Twig. Gymnosperm.
WW (1)	34	Land wall: filling of cisterns	63	OxA-failed	-	-	-	-	-	Twig. *Pinus*.
WW (1)	34	Fallen north section: upper part	75	OxA-28842	1323±26	−26.2±0.3	-	650–770	*650–720* (83%) *740–765* (12%)	Branch at least 3 years old. Gymnosperm.
WW (1)	34	Fallen north section: upper part	78	OxA-28843	1308±25	−27.1±0.3	-	650–770	*655–725* (76%) *740–770* (19%)	Twig 1 year old. Gymnosperm.
WW (1)	34	Fill of cistern 2	230	OxA-32880	1309±25	−23.5±0.3	-	650–770	*655–725* (76%) *740–770* (19%)	Two-year-old *Quercus* twig.
WW (1)	34	Fill of cistern 2	231	OxA-X-2650–48	1279±30	−27.6±0.3	-	660–780	*665–770*	One-year-old *Pinus* twig.
WW (1)	34	Fill of cistern 2	233	OxA-32881	1303±25	−25.9±0.3	-	660–770	*660–725* (74%) *740–770* (21%)	One-year-old *Pinus* twig.
WW (2)	34	Land wall	-	GrA-7987	1630±50	-	-	260–550	*355–565*	Unidentified bulk charcoal sample
WW (2)	34	Land wall: two separate pieces	52	OxA-failed	-	-	-	-	-	Branch. Probably gymnosperm.
WW (2)	34	Land wall	58	OxA-failed	-	-	-	-	-	Twig. Probably gymnosperm
WW (2)	34	Fallen north section: lower part	79	OxA-28841	1633±27	−26.6±0.3	-	350–540	*380–435* (37%) *445–540* (58%)	Twig at least 3 years old; probably *Ficus*.

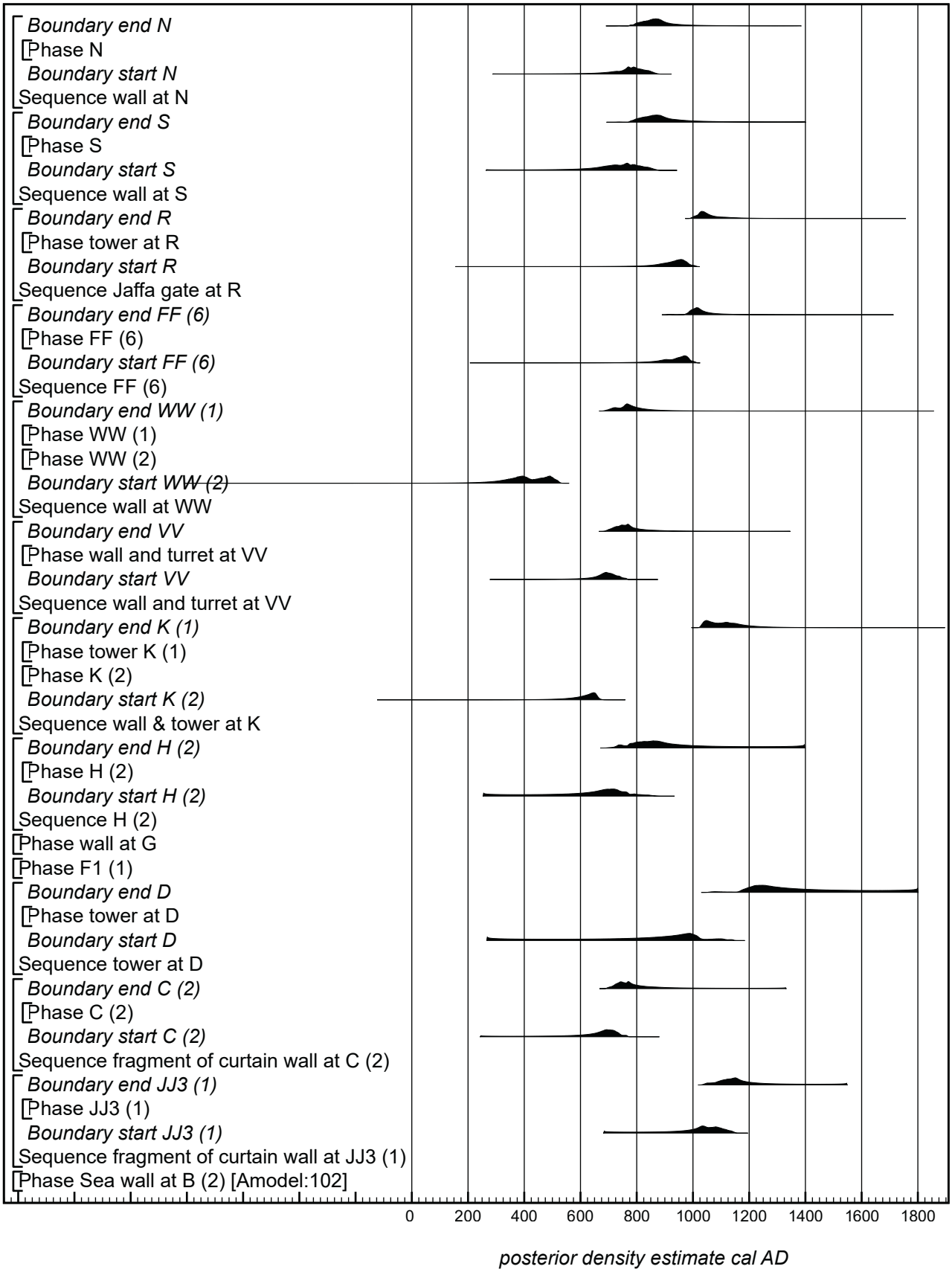

Figure 20.2. Overall Structure of model 1. The component sections are shown in figures 20.3–4. The model is defined by the OxCal keywords and by the large square brackets on the left-hand sides of figures 20.2–4 (Bronk Ramsey 2009)

as a whole is likely, given the data. In most applications, this too has a threshold value of 60.

The dates from Ashkelon are modeled in three stages. Model 1 (figures 20.2–5) attempts to determine the date of each sampled building context; model 2 (figure 20.6) groups those results from model 1 that can be shown to be of potentially the same age into building episodes; and model 3 (figure 20.7) attempts to relate these episodes to recorded construction events (table 20.2).

Model 1

The structure of model 1 is shown in figure 20.2. It makes no assumption about the relation of one wall fragment to another, treating each as an independent entity. The main prior belief incorporated is that the samples in each dated group are representative of a single episode of activity, in this case the construction of a section of wall, without necessarily including the earliest or the latest material generated by it (Buck et al. 1992). Each group is thus modeled as a phase constrained by boundaries calculated from the dates within it, a phase here meaning a group of related dates without order or sequence. The assumption, for example, that OxA-30949, OxA-31029, and OxA-31030 from triangular turret VV (figure 20.3) belong to a single phase, which had a beginning and an end, rather than that each is independent, constrains the scatter inherent in radiocarbon ages, which would otherwise make episodes of activity appear to start earlier, continue longer, and end later than they actually did (Steier and Rom 2000). At locations K and WW, where dates were obtained from successive building contexts, the two phases have been modeled as sequential. This would have provided an additional constraint had the distributions in each pair of groups overlapped. In both cases, however, the interval between the successive contexts was such that the relationships did not constrain the dates (figures 20.3–4). Where replicate measurements have been made on the same sample a weighted mean (Ward and Wilson 1978) is taken before incorporation in the model. The construction date of each building context is estimated by using the Last function in OxCal. This calculates the most recent event in a group and was chosen because the most recent dated charcoal fragment will be closest to the construction date. The resulting estimate could still be a *terminus post quem* for construction, but this becomes less probable when two or more of the measurements are statistically consistent, since this points to a single act rather than to random inclusions. At the two locations where there is only one date from a building context, B and F1 (phase 1), that date has simply been incorporated into the model. A sherd dated to A.D. 990–1050, embedded in the mortar at G, has been included as a calendar date. The model has good overall agreement (Amodel 102) and the indices of agreement for the individual dates are all adequate.

The Dated Contexts

The results of the application of model 1 for individual contexts follow the order in which they appear on the site plan in figure 20.9, counterclockwise around the circuit, from west to north.[2]

Sea wall B (phase 2), Grid 64. The only successfully dated sample probably came from older debris incorporated into the wall. It was part of a large branch, possibly *Ficus* sp. Regardless of the age of the sample, the possible reuse of the masonry makes the Byzantine-period date of *cal A.D. 420–550* (*95% probability*; figure 20.3: *OxA-30713*) a *terminus post quem* for the construction of the wall here, while pointing to Byzantine building activity of some kind nearby (not necessarily connected with the town walls).

Fragment of curtain wall JJ3 (phase 1), Grid 78. Here, two samples from branches, probably of *Pinus* sp. and *Quercus* sp., yielded statistically consistent dates (T' = 0.0; T'(5%) = 3.8; ν = 1; figure 20.3: *OxA-31024,-31025*), which provide the basis for an estimated construction date of *cal A.D. 1040–1160* (*95% probability*), probably *cal A.D. 1090–1155* (*68% probability*; figure 20.3: *build JJ3 (1)*).

Fragment of curtain wall C (phase 2), Grid 72. Only the first building phase here yielded suitable charcoal. A sample from a large branch, probably of *Quercus* sp., yielded statistically consistent replicate measurements (T' = 0.7; T'(5%) = 3.8; ν = 1), of which a weighted mean was taken before incorporation in the model (figure 20.3: *sample 10*). This is in turn statistically consistent (T' = 0.9; T'(5%) = 3.8; ν = 1) with the date for a sample from another large branch, probably of *Ficus* sp. (figure 20.3: *OxA-30945*). The two provide an estimated construction date of *cal A.D. 685–780* (*91% probability*), *cal A.D. 790–805* (*2% probability*), *cal A.D. 810–25* (*1% probability*), or *cal A.D. 840–55* (*1% probability*), probably *cal A.D. 715–55* (*50% probability*) or *cal A.D. 760–75* (*18% probability*; figure 20.3: *build C (2)*).

Tower D, Grid 75. Of the two samples here, a twig provided a tenth- to eleventh-century cal A.D. date (figure 20.3: *OxA-30556*) and a branch or log of *Pinus* sp. provided a later, twelfth- to thirteenth-century cal A.D.,

[2] For fuller descriptions, see also Chapter 19.

Table 20.2: Historically attested periods of construction and destruction.

Period	*Date AD*	*Construction*	*Destruction*
Byzantine	**ca. 324–637**		
Muslim/Umayyad	**637–750**		
	685–93	Rebuilding of walls by ʿAbd al-Malik (685–705)	
	749		Earthquake
Abbasid	**750–868**		
Tulunid	**868–905**		
Ikhshidid	**935–969**		
Fatimid	**969–1153**		
	977	Jawhar besieged in city	
	1032		Earthquake and tsunami
	1049–57	Building inscription, reign of al-Mustanṣir (1035–94)(?)	
	1068		Earthquake
	1073–94	Tower of Blood built by Badr al-Jamālī, reign of al-Mustanṣir (1035–94)	
	1150	Building of a tower under al-Ẓāfir	
	1153		Frankish siege: demolition of wall near E Gate and filling of ditches
Frankish/Crusader	**1153–87**		
	1153–87	Repairs to walls damaged in siege (assumed)	
	1187		Besieged by Saladin: destruction of walls and towers
Ayyubid	**1187–92**		
	1189	Ayyubid refortification	
	1191		Ayyubid destruction, including Tower of the Hospital and Tower of Blood (or the Templars)
Frankish/Crusader	**1192**		
	1192	Refortification by Richard I	
	1192		Deliberate destruction by Ayyubids and Franks
Ayyubid	**ca. 1195–1240**		
	1198		Deliberate destruction by Ayyubids (?)
Frankish/Crusader	**1240–47**		
	1240–41	Construction of castle by Tibald of Champagne, Hugh IV of Burgundy and Richard of Cornwall	
Ayyubid	**1247–50**		
	1247		Castle taken and destroyed by Ayyubids
Mamluk	**1250–1516**		
	1270		Deliberate destruction of castle (and town walls?) by Baybars
Ottoman	**1516–1917**		
	1775–1804		Destruction of walls for building materials by Aḥmad al-Jazzār
	1815		Excavation inside a tower by Lady Hester Stanhope
	1832–40		Destruction of walls for building materials by Ibrahim Pasha

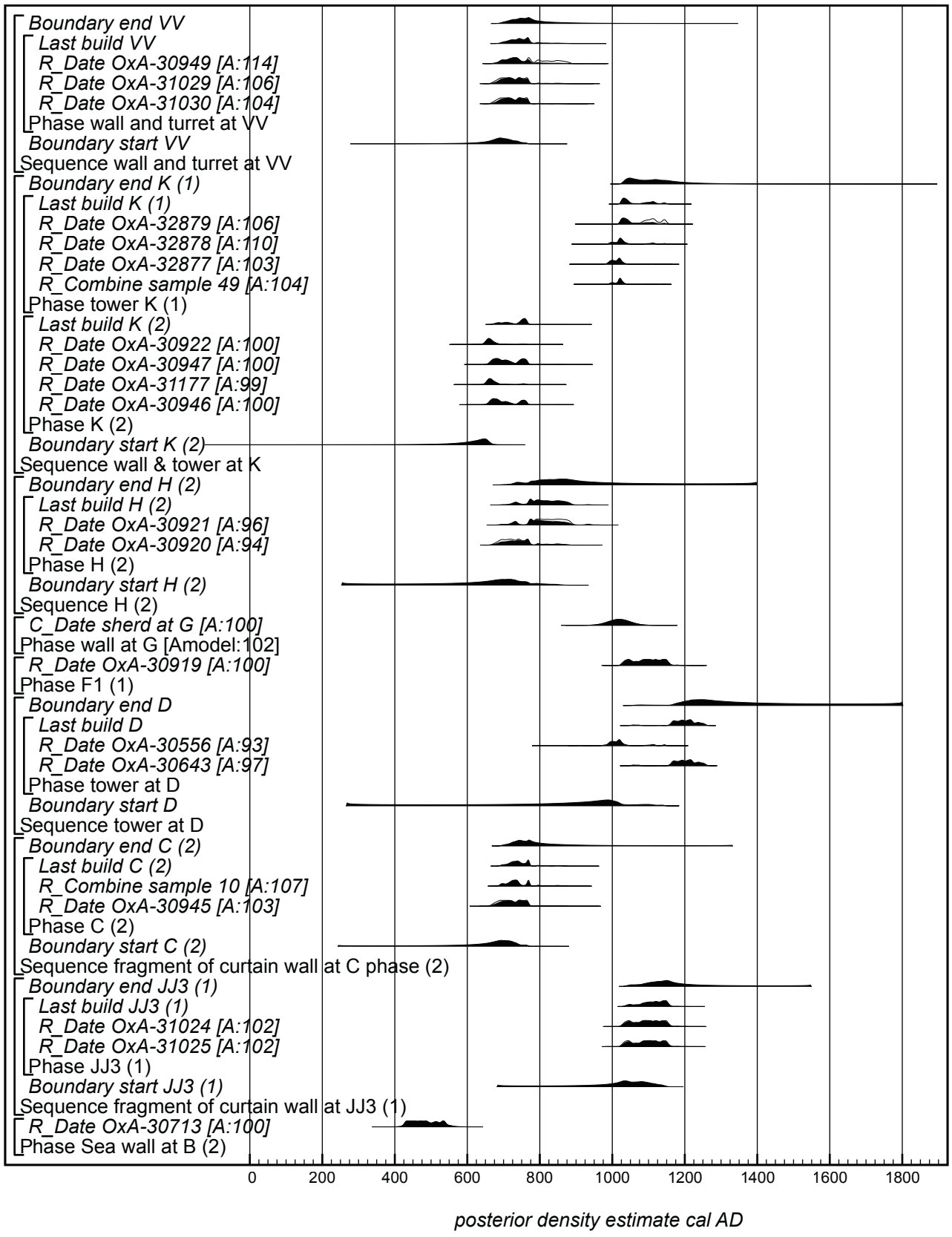

Figure 20.3. Probability distributions of radiocarbon dates for fragments of wall in the south and east of the circuit. For each date, the distribution shown in outline represents the simple radiocarbon date and the distribution shown in solid black is derived from and constrained by the model. Other distributions represent parameters estimated by the model, for example "*build JJ (1)*." The model is defined by the OxCal keywords (Bronk Ramsey 2009) and by the large square brackets down the left-hand side of figures 20.2–4. The numbers in square brackets which follow the dates, for example, '*OxA-30713 [A:100]*', are individual indices of agreement.

date (figure 20.3: *OxA-30643*). The first sample was clearly residual; the second provides the basis for an estimated construction date of *cal A.D. 1055–65* (*1% probability*) or *cal A.D. 1155–1265* (*94% probability*), probably *cal A.D. 1165–1225* (*68% probability*; figure 20.3: *build D*).

Fragment of a feature attached to the inside face of the town wall F1 (phase 1), Grid 62. Samples could be collected only from the later phase here. Two out of three failed to date. The remaining one, an olive (*Olea europaea*) stone, provided a date of *cal A.D. 1025–1160* (*95% probability*), probably *cal A.D. 1035–55* (*12% probability*) or *cal A.D. 1080–1155* (*56% probability*; figure 20.3: *OxA-30919*).

Fragment of curtain wall with possible abutment of tower G (phase 1), Grid 56. While no samples were dated from here, a *terminus post quem* for construction is provided by small sherd of Fustat Fatimid *sgraffiato* of the late tenth to eleventh century. This is incorporated into the model as a calendar date of A.D. 990–1050 (figure 20.3: *sherd at G*).

Fragmentary remains of a tower and wall H (phase 2), Grid 49. Two samples from the tower itself (phase 1) failed to date. Fragments from two large branches or logs of *Pinus* sp. from the wall to which it was attached (phase 2) both provided dates. The more mature, estimated as at least seven years old, dated to the seventh to ninth centuries cal A.D. (figure 20.3: *OxA-30920*); the less mature, estimated as at least four years old, dated to the eighth to ninth centuries cal A.D. (figure 20.3: *OxA-30921*). On the basis of this more recent date, the wall would have been built in *cal A.D. 715–55* (*11% probability*) or *cal A.D. 760–890* (*84% probability*), probably *cal A.D. 770–865* (*68% probability*; figure 20.3: *build H (2)*).

D-shaped tower and adjoining curtain wall K, Grid 41. No samples were collected from the first building phase here (phase 4), and two from the second phase (phase 3) failed to date. From phase 2, the rebuilding of the town wall, three samples of *Pinus* sp., one a twig and two from branches or logs (figure 20.3: *OxA-30922, -30947, -31177*), together with an otherwise unidentified twig from a deciduous tree or shrub (figure 20.3: *OxA-30946*), all yielded statistically consistent measurements (T' = 2.4; T'(5%) = 7.8; ν = 3). These provide the basis for an estimated construction date of *cal A.D. 670–730* (*40% probability*) or *cal A.D. 735–70* (*55% probability*), probably *cal A.D. 685–90* (*4% probability*) or *cal A.D. 700–20* (*14% probability*) or *cal A.D. 740–70* (*50% probability*; figure 20.3: *build K (2)*).

The phase 1 tower built onto the wall provided four samples, all twigs, one identified as *Quercus* sp. and another as probably *Olea europaea*. Replicate measurements on discrete fragments from one sample (figure 20.3: *OxA-30969, -30970*) are statistically inconsistent at 95% confidence but consistent at 99% confidence (T' = 6.4; T'(5%) = 3.8; ν = 1). A weighted mean is therefore taken before inclusion in the model. These and the remaining three measurements (figure 20.3: *OxA-32877 to -32879*) are all statistically consistent (T' = 2.0; T'(5%) = 78; ν = 3) and provide the basis for an estimated construction date of *cal A.D. 1020–70* (*57% probability*) or *cal A.D. 1075–1130* (*32% probability*) or *cal A.D. 1135–55* (*6% probability*), probably *cal A.D. 1020–50* (*50% probability*) or *cal A.D. 1095–1120* (*18% probability;* figure 20.3: *build K (1)*).

Triangular turret VV, Grid 34. Two twig samples (figure 20.3: *OxA- 30949, -31029*) and a third from a branch (figure 20.3: *OxA-31030*) from the single-build wall and turret here yielded statistically consistent measurements (T' = 0.9; T'(5%) = 6.0; ν = 2). These provide an estimate for the construction of the wall and turret of *cal A.D. 685–830* (*94% probability*) or *cal A.D. 845–55* (*1% probability*), probably *cal A.D. 715–75* (*68% probability*; figure 20.3: *build VV*).

Curtain wall WW, Grid 34. The earlier wall here (phase 2) was the context of a bulk charcoal sample dated in the 1970s (figure 20.4: *GrA-7987*; Kedar and Mook 1978). This is statistically consistent with a measurement on a single twig fragment (figure 20.4: *OxA-28841*; T' = 0.0; T'(5%) = 3.8; ν = 1). Further short-life samples were elusive, but these two dates provide the basis for an estimated construction date of *cal A.D. 395–555* (*95% probability*), probably *cal A.D. 410–25* (*7% probability*) or *cal A.D. 490–540* (*61% probability*; figure 20.4: *build WW (1)*).

The later contexts (phase 1) yielded five twig samples, two from the upper part of collapsed wall fragment 9 (figure 20.4: *OxA-28842*, *-28843*) and three from the masonry fill of cistern 2 (figure 20.4: *OxA-32880*, *-32881*, *OxA-X-2650–48*). The last of these was given an 'OxA-X' number because it was a research measurement made using nonstandard or experimental methods. All five are statistically consistent (T' = 1.3; T'(5%) = 9.5; ν = 4) and provide the basis for an estimated construction date of *cal A.D. 680–775* (*95% probability*), probably *cal A.D. 700–20* (*15% probability*) or cal A.D. *740–70* (*53% probability*; figure 20.4: *build WW (1)*).

Tower FF, Grid 20. Despite excavation here, only part of the phase 6 wall (context 90) yielded datable

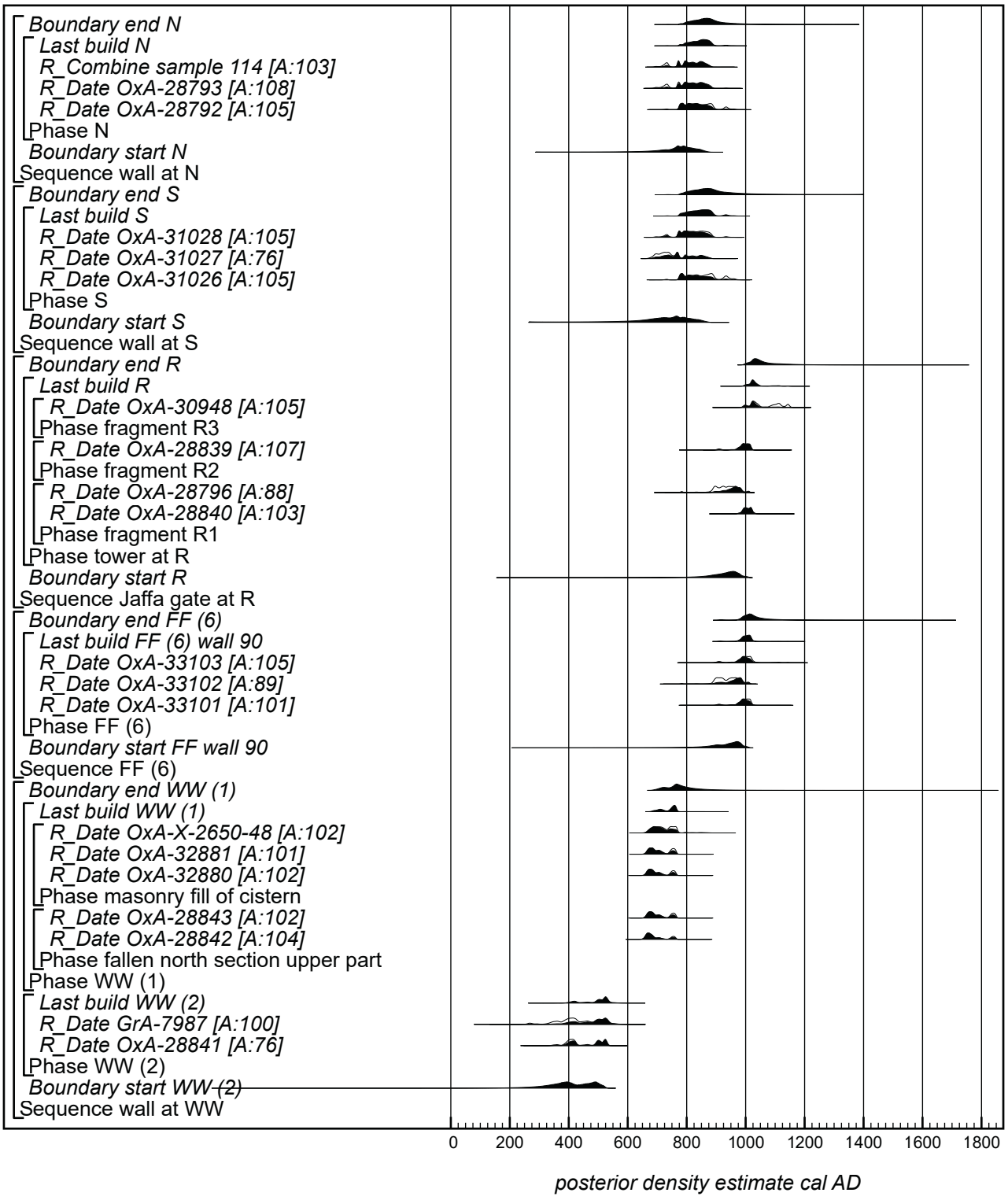

Figure 20.4. Probability distributions of radiocarbon dates for fragments of wall in the northeast and north of the circuit. The format is the same as in figure 20.3

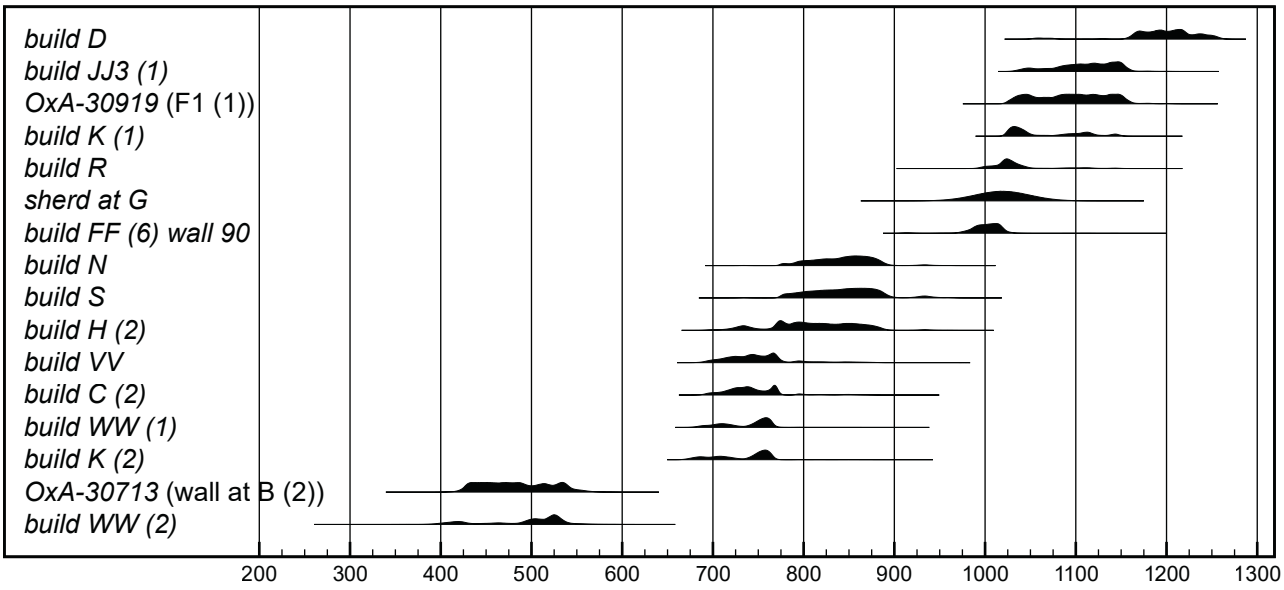

Figure 20.5. A summary of construction dates for building contexts estimated by model 1 (table 20.4)

Table 20.3: Column 2: results of $\chi 2$ tests on single radiocarbon measurements or the weighted means of replicates for samples from wall fragments apparently of similar date. Column 3: results of the Combine operation on the highest posterior density intervals for construction estimates derived from model 1.

Wall fragments	*Are individual radiocarbon determinations statistically consistent?*	*May highest posterior density intervals for estimated construction dates be combined?*	*Episode (Fig. 6)*
B (2)	Yes	Yes	Group one
WW (2)	n=3	n=2	
	T'=4.1; T'(5%)=6.0; ν=2	Acomb=103.6% (An= 50.0%)	
C (2)	Yes, at 99%	Yes	Group two
K (2)	n=14	n=4	
VV	T'=25.0; T'(5%)=22.4; ν=13	Acomb=148.8% (An= 35.4%)	
WW (1)			
H (2)	Yes	Yes	Group three
S	n=8	n=3	
N	T'=9.9; T'(5%)=14.1; ν=7	Acomb=117.1% (An= 40.8%)	
G (1)	Yes, if the oldest date (OxA-28786) is excluded	Yes	Group four
K (1)	n=6	n=4	
FF (6) Wall 90	T'=10.7; T'(5%)=11.1; ν=5	Acomb= 90.7% (An= 35.4%)	
R			
JJ3 (1)	Yes	Yes	Group five
F1 (1)	n=7	n=2	
	T'=11.1; T'(5%)=12.6; ν=6	Acomb=108.6% (An= 50.0%)	

Table 20.4: Estimated Parameters for Events Derived from Models 1, 2 and 3

	Model 1 (Figs. 2–5)		*Model 2 (Fig. 6)*		*Model 3 (Fig. 7)*	
Parameter	*cal AD 95% probability.*	*cal AD 68% probability*	*cal AD 95% probability*	*cal AD 68% probability*	*cal AD 95% probability*	*cal AD 68% probability*
start one	-	-	*400–535*	*415–510*	*395–525*	*415–495*
build WW (2)	*395–555*	*410–425* (7%)	*395–555*	*410–430* (7%)	-	-
		490–540 (61%)		*490–540* (61%)		
OxA-30713 (wall at B (2))	*420–550*	*430–495* (55%)	*420–550*	*430–495* (55%)	-	-
		510–520 (5%)		*510–520* (5%)		
		525–540 (8%)		*525–540* (8%)		
end one	-	-	*435–565*	*495–545*	*455–570*	*500–545*
start two	-	-	*685–765*	*700–755*	*690–765*	*700–755*
build K (2)	*670–730* (40%)	*685–690* (4%)	*680–775*	*740–770*	-	-
	735–770 (55%)	*700–720* (14%)				
		740–770 (50%)				
build WW (1)	*680–775*	*700–720* (15%)	*695–775*	*740–770*	-	-
		740–770 (53%)				
build C (2)	*685–780* (91%)	*715–755* (50%)	*690–780* (89%)	*720–775*	-	-
	790–805 (2%)	*760–775* (18%)	*790–825* (4%)			
	810–825 (1%)		*840–860* (2%)			
	840–855 (1%)					
build VV	*685–830* (94%)	*715–775*	*690–830* (93%)	*720–775*	-	-
	840–855 (1%)		*840–860* (2%)			
end two	-	-	*735–870*	*745–780* (67%)	*735–810*	*755–775*
				795–800 (1%)		
start three	-	-	*720–755* (9%) *760–865* (86%)	*770–835*	*765–855*	*770–825*
build H (2)	*715–755* (11%)	*770–865*	*720–755* (9%)	*770–865*	-	-
	760–890 (84%)		*760–890* (86%)			
build N	*775–895*	*815–885*	*775–895*	*815–885*	-	-
build S	*770–900* (93%)	*810–890*	*770–900* (93%)	*810–890*	-	-
	925–940 (2%)		*925–940* (2%)			
end three	-	-	*805–905* (90%)	*845–890*	*815–905* (90%)	*845–890*
			920–950 (5%)		*920–950* (5%)	
start four	-	-	*955–1030*	*980–1015*	*955–1030*	*980–1015*
build FF (6) Wall 90	*965–1035*	*990–1020*	*965–1035*	*990–1020*	-	-
sherd at G	*955–1080*	*990–1050*	*955–1080*	*990–1055*	-	-
build R	*990–1060* (86%)	*1005–1045*	*990–1060* (86%)	*1005–1045*	-	-
	1080–1125 (9%)		*1080–1125* (9%)			
build K (1)	*1020–1070* (57%)	*1020–1050* (50%)	*1020–1070* (57%)	*1020–1055* (50%)	-	-
	1075–1130 (32%)	*1095–1120* (18%)	*1075–1130* (32%)	*1095–1120* (18%)		
	1135–1155 (6%)		*1135–1155* (6%)			

end four	-	-	*1020–1130* (88%) *1135–1155* (7%)	*1025–1055* (39%) *1090–1125* (29%)	*1020–1110*	*1025–1055*
start five	-	-	*1025–1145*	*1030–1115*	*1035–1140*	*1045–1055* (9%) *1065–1125* (59%)
OxA-30919 (F1 (1))	*1025–1160*	*1035–1055* (12%) *1080–1155* (56%)	*1025–1160*	*1035–1055* (12%) *1080–1155* (56%)	-	-
build JJ3 (1)	*1040–1160*	*1090–1155*	*1040–1160*	*1090–1155*	-	-
end five	-	-	*1055–1170*	*1105–1160*	*1085–1165*	*1115–1160*
build D	*1055–1065* (1%) *1155–1265* (94%)	*1165–1225*	*1055–1065* (1%) *1155–1250* (94%)	*1165–1225*	*1160–1245*	*1165–1225*

short-life samples, comprising seeds, leaves, and twig charcoal (figure 20.4: *OxA-33101* to *-33103*). All three results are statistically consistent (T' = 3.5; T'(5%) = 6.0; ν = 2); they provide the basis for a construction date of *cal A.D. 965–1035* (*95% probability*), probably *cal A.D. 990–1020* (*68% probability*; figure 20.4: *build FF (6) wall 90*).

Jaffa Gate R, Grid 11. Dates were obtained for a twig and a branch sample from fragment R1 (figure 20.4: *OxA-28796*, *-28840*), a twig sample from fragment R2 (figure 20.4: *OxA-28839*), and a branch sample from fragment R3 (figure 20.4: *OxA-30948*). Three of the four measurements are statistically consistent (T' = 3.4; T'(5%) = 6.0; ν = 2), the exception being the measurement for the branch sample from fragment R1, which may have been more mature than the rest (figure 20.4: *OxA-28796*). The estimated construction date is *cal A.D. 990–1060* (*86% probability*) or *cal A.D. 1080–1125* (*9% probability*), probably *cal A.D. 1005–45* (*68% probability*; figure 20.4: *build R*).

Curtain wall S, Grid 2. From the upper wall here came two twig samples (figure 20.4: *OxA-31027*, *-31028*) and one sample from a branch or log (figure 20.4: *OxA-31026*). Measurements on all three are statistically consistent (T' = 4.4; T'(5%) = 6.0; ν = 2) and point to a construction date of *cal A.D. 770–900* (*93% probability*) or *cal A.D. 925–40* (*2% probability*), probably *cal A.D. 810–90* (*68% probability*; figure 20.4: *build S*).

Fragment of wall N, Grid 1. Replicate measurements on a twig sample were statistically inconsistent at 95% confidence but consistent at 99% (T' = 4.0; T'(5%) = 3.8; ν = 1). A weighted mean was taken before incorporation in the model (figure 20.4: *sample 114*). This is statistically consistent with two measurements on branch samples (figure 20.4: *OxA-28792*, *-28793*). Together they provide an estimated construction date of *cal A.D. 775–895* (*95% probability*), probably cal A.D. *815–85* (*68% probability*; figure 20.4: *build N*).

Results of model 1

The high frequency of statistically consistent dates from individual building contexts indicates that very little redeposited charcoal or significantly mature wood was incorporated in the mortars. Figure 20.5 summarizes the construction estimates calculated by model 1, which are listed in table 20.4. They compare well with our general predictions as to date ranges and are fully consistent with the relative phasing indicated by archaeological and structural analysis. Some estimates are more robust than others. The strongest are those where there are at least three statistically consistent results, at least some of them on short-life samples: e.g., K (phases 1 and 2), VV, WW (phase 1), FF (phase 6, wall 90), R, /S, and N. The most questionable are those where the date rests on a single charcoal or charred plant sample, as at B and F1 (phase 1), or on a single incorporated sherd as at G. In these cases there is no way of checking whether the charcoal or sherd was already old when incorporated, with the result that the actual construction date could have been later.

Synthesis

So far, fragments of wall in different areas have been treated as separate entities. Figure 20.5, however, suggests that there are possible groupings among the building contexts. These can be explored using two functions in OxCal. The R_Combine function, already used to test the statistical consistency of replicate

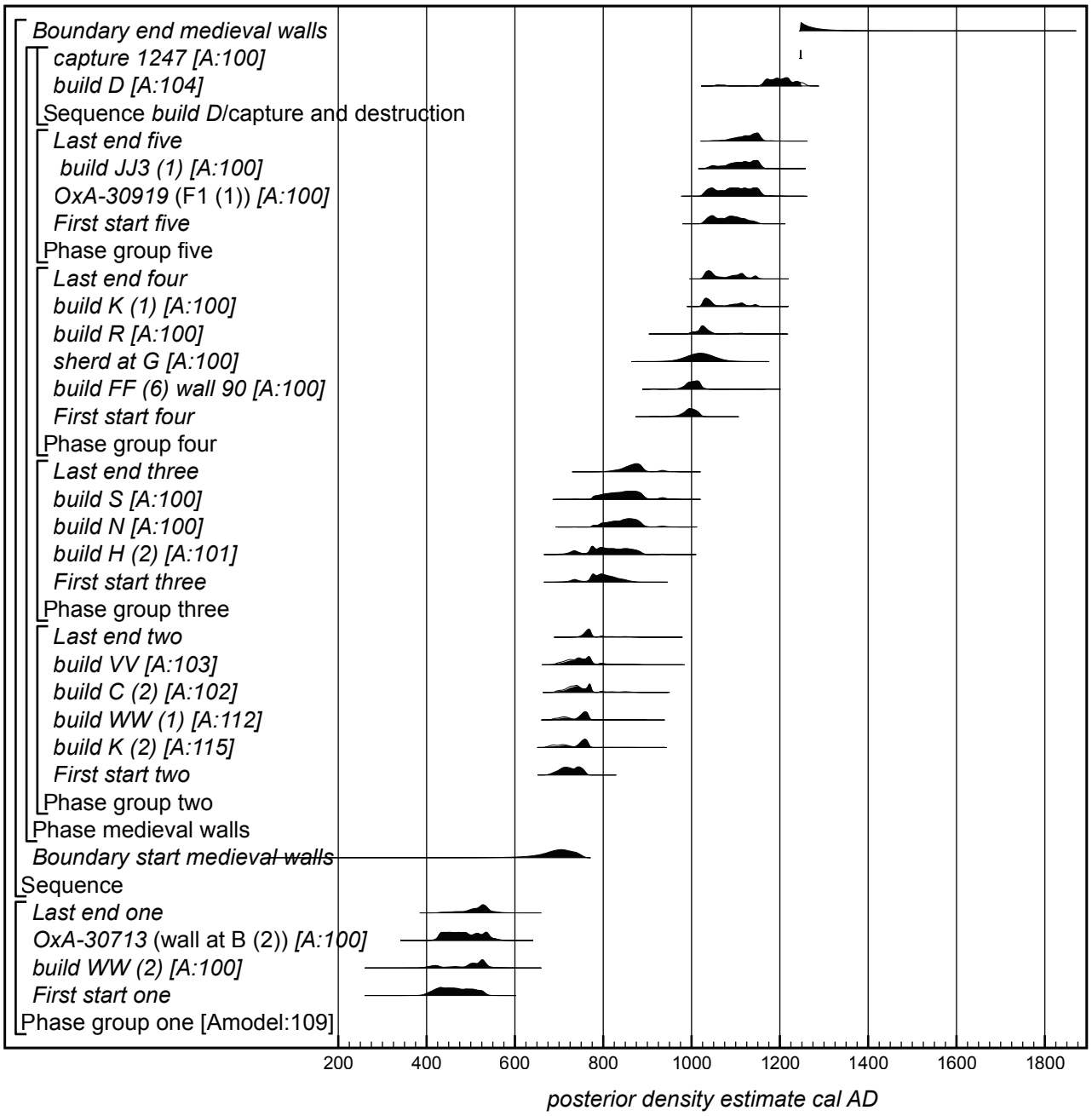

Figure 20.6. Model 2: Estimated construction dates for building contexts derived from model 1, modeled in phases based on the calculations summarized in table 20.3. The format is the same as in figure 20.3.

measurements and of determinations from the same building context by means of χ^2 tests, is now applied to all the individual measurements (or weighted means in the case of replicates) from groups of building contexts which are close to each other in age. The Combine function combines posterior density functions which give independent information on a parameter, in this case a potential episode of building, and calculates a combination agreement index, Acomb, which is used to test if distributions may indeed be combined, the acceptable threshold (An) being $1/\sqrt{(2n)}$, so that the distributions may be combined if Acomb is equal to or greater than An. This is here applied to the construction estimates for building contexts which appear close to each other in age (groups one to five). The results of this exercise are summarized in table 20.3. Both indicate that, for example, the building contexts making up group three, H (phase 2), N, and S, could

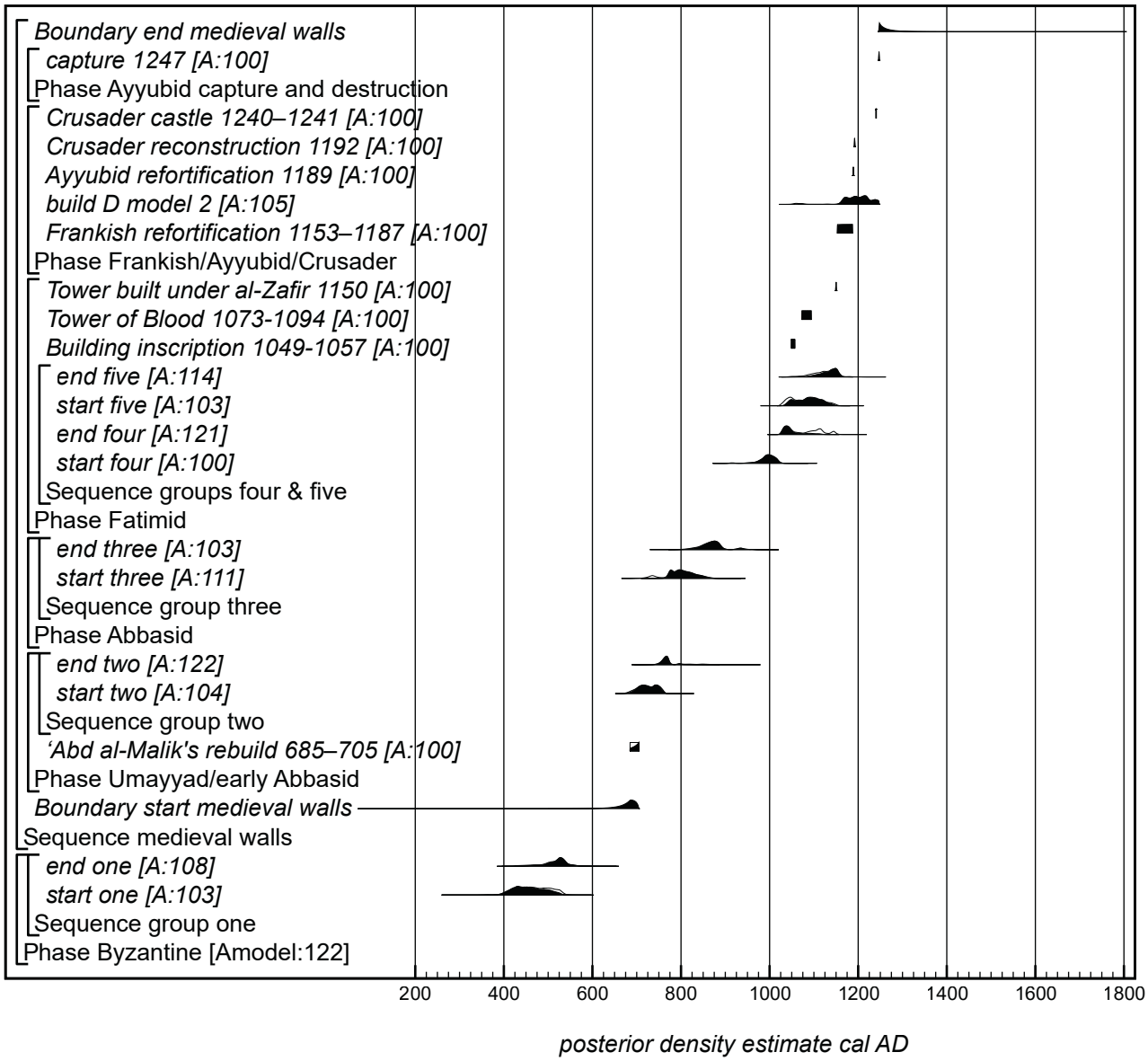

Figure 20.7. Model 3: Estimated start and end dates for groups of building contexts, derived from model 2, modeled in historical phases with documented construction dates (table 20.2). The format is the same as in figure 20.3.

all belong to a single episode of construction, although it does not demonstrate that they actually did. When alternative groupings are attempted, such as a merger of groups four and five, both indices of agreement become too low.

Model 2

On this basis, model 2 treats each group of construction estimates defined in table 20.3 as a phase, leaving the single later estimate *build D* to stand alone, constrained to be earlier than the Ayyubid capture and destruction of 1247, after which no construction is documented or likely. Groups two to five and *build D* are modeled as parts of a single, more or less continuous phase of activity, without any assumption that they were necessarily sequential. Group one, comprising B (phase 2) and WW (phase 2), is kept apart from this because of the length of the interval between it and group two. Constraint and precision are slightly increased (figure 20.6) and it becomes possible to calculate intervals between groups. This model has good overall agreement (Amodel 109) and all the individual indices of agreement are adequate. Estimates for the start and end date of each group and for the intervals between them are listed in tables 20.4 and 20.5.

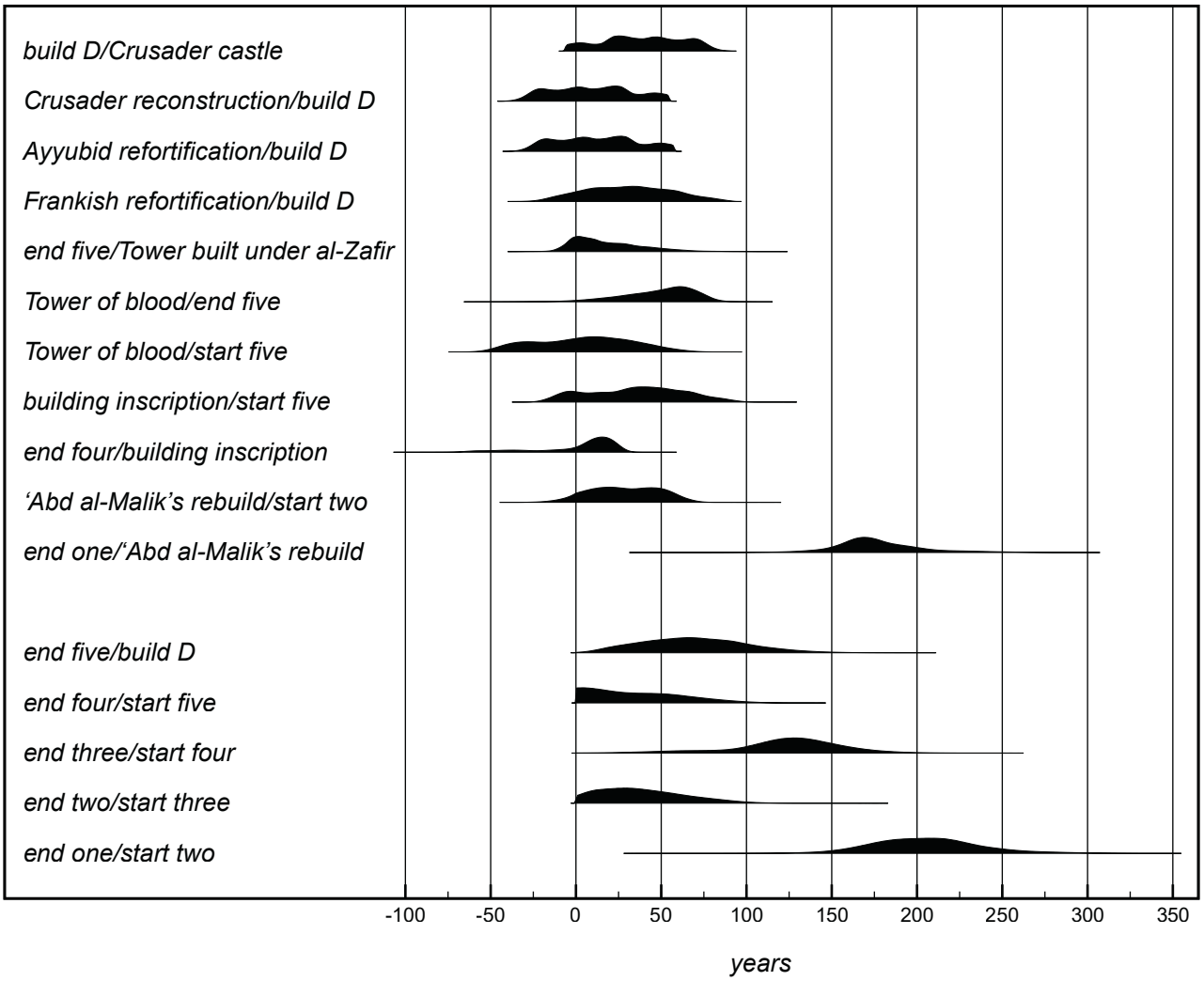

Figure 20.8. Intervals between the episodes of construction, and between them and historically documented construction events, derived from model 3 (figure 20.7, table 20.5). The negative part of each distribution represents overlap.

Model 3

Two reasons for the imprecision of the estimates in model 2 are: (1) that each is based on relatively few dates, one effect of which is that start and end estimates for a group can overlap; and (2) that there is no assumption of sequence between groups, so that they too can overlap. In model 3 both the start and end estimates for each group and the groups themselves are constrained to be sequential, except for group 1, which is again kept apart from the rest of the sequence because of the length of the interval between it and the rest (figure 20.7).

Model 3 also attempts to relate these estimates to the historical record (table 20.2). This is a challenging task, given the difference in precision between Highest Posterior Density Intervals and historical dates and the fact that there are radiocarbon dates for only some 25 percent of the identified building contexts. It is compounded by the inexact nature of some of the historical dates and by the consideration that historical sources, especially those of a narrative nature, may not provide a full tally of constructions and destructions: not all such building works are likely to be mentioned in surviving records; individual episodes, especially those relating to specific buildings or historical incidents, are more likely to be recorded than general programs of maintenance and rebuilding continuing over many years; and, in describing military action, medieval authors, whether writing from the winning or losing side, have a tendency to exaggerate the extent of destruction and consequent repair of fortifications. Furthermore, what survives today of Ashkelon's medieval defenses represents only a small

Table 20.5: Estimated Intervals between Events Derived from Models 2 and 3. Where an estimate is partly or wholly negative, this reflects overlap between the two parameters concerned.

	Model 2 (Fig. 20.6)		*Model 3 (Fig. 20.7)*	
Interval	*Duration in years (95% probability)*	*Duration in years (68% probability)*	*Duration in years (95% probability)*	*Duration in years (68% probability)*
end one/start two	*+140 to +295*	*+165 to +240*	*+140 to +275*	*+170 to +235*
end two/start three	*−80 to +105*	*−35 to −20 (6%)*	*−5 to +90*	*+5 to +55*
		−5 to + 75 (62%)		
end three/start four	*+45 to +195*	*+100 to +165*	*+45 to +185*	*+100 to +160*
end four/start five	*−90 to +100*	*−45 to +65*	*0 to +90*	*0 to +50*
end five/build D	*−85 to −65 (1%)*	*+30 to +110*	*+10 to +130*	*+30 to +100*
	−5 to +170 (94%)			
end one/ʿAbd al-Malik's rebuild	-	-	*+125 to +245*	*+150 to +195*
ʿAbd al-Malik's rebuild/start two	-	-	*−10 to +70*	*+5 to +55*
end four/building inscription	-	-	*−55 to +35*	*−5 to +30*
building inscription/start 5	-	-	*−20 to +85*	*−10 to +5 (9%)*
				+15 to +70 (59%)
Tower of Blood/start five	-	-	*−50 to +55*	*−35 to +25 (9%)*
				−20 to +40 (59%)
Tower of Blood/end five	-	-	*1 to +85*	*+35 to +75*
end five/Tower built under al-Ẓāfir	-	-	*−15 to +65*	*−10 to +30*
Frankish refortification/build D	-	-	*−20 to +80*	*+1 to +60*
Ayyubid refortification/build D	-	-	*−30 to +60*	*−25 to +35*
Crusader reconstruction/build D	-	-	*−30 to +55*	*−25 to +30*
build D/Crusader castle	-	-	*−5 to +80*	*+15 to +75*

fraction of what must once have existed, with large areas of the enceinte now devoid of any upstanding masonry at all, and as explained above, many of the surviving parts failed to produce suitable samples; it is therefore quite possible that entire building phases will be unrepresented in the data discussed here. With these reservations, model 3 places the dates of documented construction episodes in the same phases as the starts and ends of groups of building contexts calculated by model 2, although not in any sequence with those starts and ends (figure 20.7). This model too has good overall agreement (Amodel 122) and all the individual indices of agreement are adequate. The narrative which follows employs parameters from model 3. The dated building contexts are shown on the site plan in figure 20.9.

Group one (WW, phase 2) and the structure from which the reused masonry at B came), with its fifth- to sixth-century date (figure 20.7: *start one*, *end one*) is clearly Byzantine, a period to which other wall fragments can be attributed on archaeological grounds.[3] There is no dated construction between this and ʿAbd al-Malik's historically attested refortification, which began sometime between A.D. 685 and 693, *125–245 years* later (*95% probability*), probably *150–195 years* later (*68% probability*; figure 20.8: *end one/ʿAbd al-Malik's rebuild*), and may have continued until his death in 705 or even later. This rebuilding overlaps with the start of group two, in *cal A.D. 690–765* (*95% probability*), probably in *cal A.D. 700–55* (*68% probability*; figure 20.7: *start two*). Most of the span of group two falls in the Umayyad period, with a thin tail of probability extending past the mid-eighth century cal A.D. into the Abbasid period (figure 20.7: *end two*). The overlap between ʿAbd al-Malik's reconstruction and the start of group two is, however, slight. It is *92% probable* (table 20.6) that his reconstruction preceded the start of group two, the estimated interval between

[3] See Chapter 19.

Table 20.6. An Ordering of Key Parameters from Post-Byzantine Contexts Derived from Model 3 and of Documented Construction Episodes. Each cell expresses the % probability that the event in the first column is earlier than the event in the subsequent columns. It is, for example, 85% probable that ʾAbd al-Malik's rebuild of 685–693 preceded the start of group two.

	ʾAbd al-Malik's rebuild 685–705	*start two*	*end two*	*start three*	*end three*	*start four*	*end four*	Building inscription 1049–1057	Tower of Blood 1073–1094	*start five*	*end five*	Tower built under al-Ẓāfir 1150	Frankish refortification 1153–1187	*build D*	Ayyubid refortification 1189	Crusader reconstruction 1192	Crusader castle 1240–1241
ʾAbd al-Malik's rebuild 685–705	-	92	100	100	100	100	100	100	100	100	100	100	100	100	100	100	100
start two		-	100	100	100	100	100	100	100	100	100	100	100	100	100	100	100
end two			-	100	100	100	100	100	100	100	100	100	100	100	100	100	100
start three				-	100	100	100	100	100	100	100	100	100	100	100	100	100
end three					-	100	100	100	100	100	100	100	100	100	100	100	100
start four						-	100	100	100	100	100	100	100	100	100	100	100
end four							-	70	86	100	100	100	100	100	100	100	100
Building inscription 1049–1057								-	100	86	100	100	100	100	100	100	100
Tower of Blood 1073–1094									-	57	98	100	100	100	100	100	100
start five										-	100	100	100	100	100	100	100
end five											-	81	100	100	99	99	100
Tower built under al-Ẓāfir 1150												-	100	100	100	100	100
Frankish refortification 1153–1187													-	88	100	100	100
build D														-	33	38	95
Ayyubid refortification 1189															-	100	100
Crusader reconstruction 1192																-	100
Crusader castle 1240–1241																	-

them being *−10 to +70 years* (*95% probability*), probably *5 to 55 years* (*68% probability*; figure 20.8: *ʿAbd al-Malik's rebuild/start 2*). In other words, the construction of the towers and lengths of wall making up group two, comprising C (phase 2), K (phase 2), VV, and WW (phase 1), could postdate this major documented refortification. In view of the fragmentary nature of the surviving evidence this is not particularly surprising, and supports the idea that the program of building works initiated by ʿAbd al-Malik continued after A.D. 705.

Group two ended in *cal A.D. 735–810* (*95% probability*), probably *cal A.D. 755–75* (*68% probability*; figure 20.7: *end two*), almost certainly before the start of group three in *cal A.D. 765–855* (*95% probability*), probably in *cal A.D. 770–825* (*68% probability*; figure 20.7: *start three*), the estimated interval between them being *−5 to +90 years* (*95% probability*), probably *5 to 55 years* (*68% probability*; figure 20.8: *end two/start three*). The whole span of group three, comprising H (phase 2), S, and N, falls in the Abbasid period and does not correspond to any historically documented

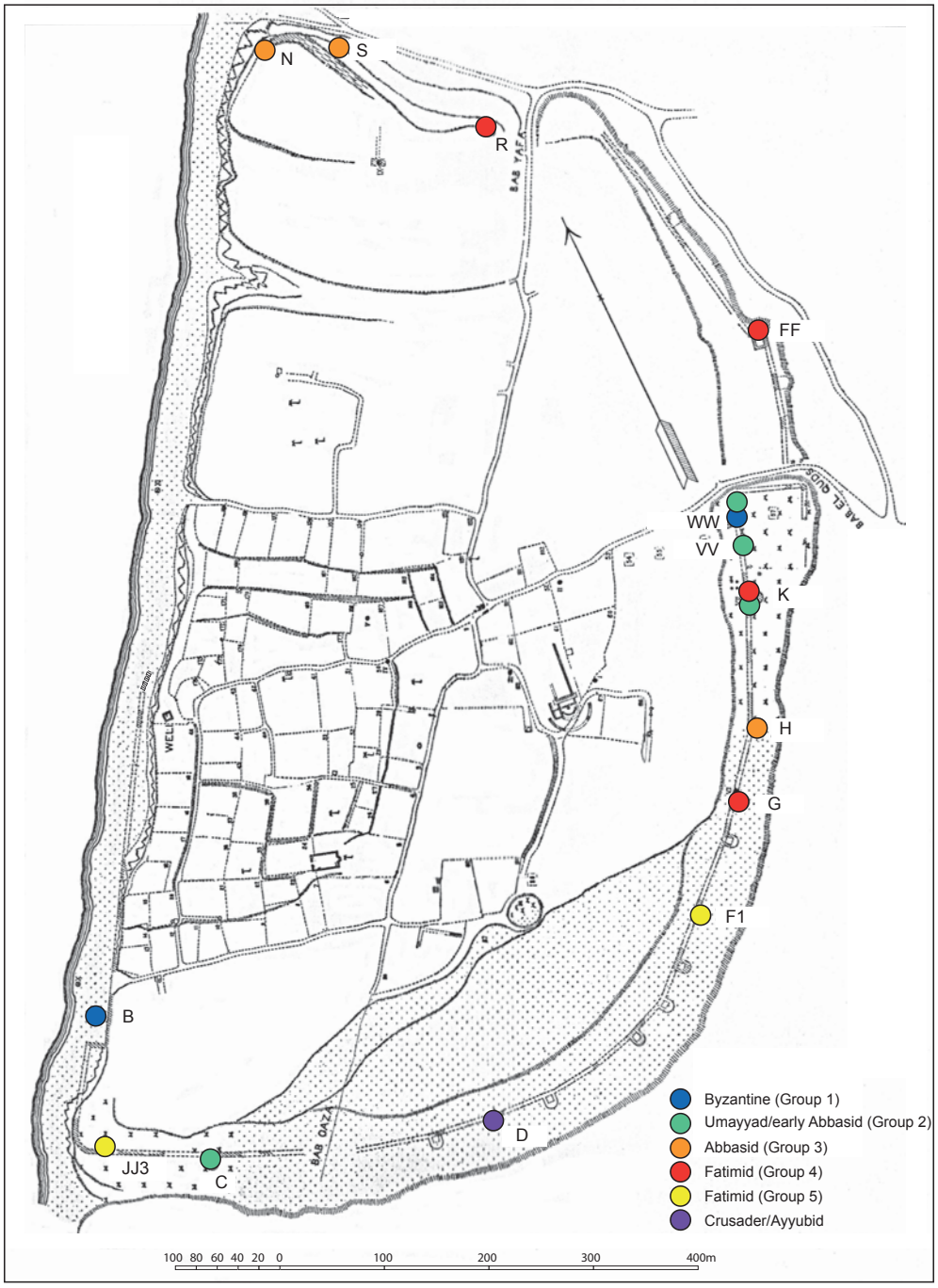

Figure 20.9. Plan of Ashkelon showing dated contexts.

construction work. An interval of *45 to 185 years* (*95% probability*), probably *100 to 160 years* (*68% probability*; figure 20.8: *end three/start four*) separated the end of group three in *cal A.D. 815–905* (*90% probability*) or *cal A.D. 920–50* (*5% probability*), probably *cal A.D. 845–90* (*68% probability*; figure 7: *end three*) from the start of group four in *cal A.D. 955–1030* (*95% probability*), probably *cal A.D. 980–1015* (*68% probability*; figure 20.7: *start four*). From a historical perspective, group three is perhaps best seen as a resumption of the building program begun under ʿAbd al-Malik, after a period of political uncertainty resulting from the overthrow and assassination of al-Walid II in 744 and the establishment of the Abbasid dynasty from 750 onward. It also suggests that, despite the greater attention that the early Abbasids paid

to the eastern provinces than to Syria and Palestine, the security of the Mediterranean coastline continued to be taken as seriously under the Abbasids as it had under the Umayyads.

The spans of group four, comprising G (phase 1), K (phase 1), FF (phase 6, wall 90), and R, and group 5, represented by JJ3 (phase 1) and F1 (phase 1), both fall in the Fatimid period, the later part of which corresponds to a plateau in the calibration curve in the late eleventh to mid-twelfth century A.D. (figure 20.1). The greatest difference between models 2 and 3 is in the estimates for the end of group 4 and the start of group 5 and hence for the interval between them (tables 20.4–5). In model 2, the estimated interval is *−90 to +100 years* (*95% probability*), probably *−45 to +65 years* (*68% probability*; table 20.5); in other words, they may equally have overlapped or have been separated by a few decades. In model 3, where they are constrained to be successive, that interval is *0 to +90 years* (*95% probability*), probably *0 to +50 years* (*68% probability*; figure 20.8: *end four/start five*), so that they could have been immediately consecutive or separated by up to half a century. Both models have good agreement, so either may be correct. Groups four and five both overlap with two documented constructions: building work in the reign of al-Mustansir in A.D. 1049–57, and the construction of the Tower of Blood by Badr al-Jamali in A.D. 1073–94 (table 20.2). These could each correspond to either group, though more probably group five than four (figures 20.7–8, table 20.5). It is *81% probable* (table 20.6) that group five was complete before a final documented Fatimid construction, that of a tower built under al-Zafir in A.D. 1150, the interval between the end of group five and A.D. 1150 being *−15 to +65 years* (*95% probability*), probably *−10 to +30 years* (*68% probability*; figure 20.8: *end five/tower built under al-Zafir*).

A mid-twelfth- to mid-thirteenth-century cal A.D. estimate for the construction of a tower at D in the south of the circuit (figure 20.7: *build D*) is the latest in the series and is effectively based on a single date (figure 20.3: *OxA-30643*) because the second date from this context is much older (figure 20.3: *OxA-30556*). It can to some extent be related to the successive changes of control in this period (table 20.2). It is *88% probable* (table 20.6) that it postdates the Frankish refortification likely to have taken place in 1153–87, the estimated interval between them being *−20 to +80 years* (*95% probability*), probably *1–60 years (68% probability*; figure 20.8: *Frankish refortification/build D*). It is *95% probable* (table 20.6) that the tower predates the construction of the Crusader castle in A.D. 1240–41, the estimated interval between them being *−5 to +80 years* (*94% probability*), probably *15–75 years* (*68% probability*; figure 20.8: *build D/Crusader castle*). In the intervening period, it could correspond to the Ayyubid refortification of 1189, to the Crusader refortification of 1192, or to an undocumented event.

Conclusions

The salient point to emerge from the analysis is that all but one of the dated building episodes predate the Crusader possession of the city, ranging from Byzantine to Fatimid in date, and that even the remaining one could be Ayyubid. Other Crusader work is undoubtedly present, notably in the castle, from which no suitable samples could be recovered, but, in terms of this project's sampling, the circuit is essentially earlier. The incomplete correspondence between documented and radiocarbon-dated building episodes highlights the fragmentary nature both of the historical record of building activity and of the surviving physical evidence itself. Notable examples include the undocumented construction of lengths of wall in the eighth to ninth centuries cal A.D. (group three) at H (phase 2), S, and N, and the historically attested building of a tower in A.D. 1150, for which there is as yet no physical evidence. It is not impossible that some of these lacks of correspondence may eventually be bridged by future documentary or epigraphic discoveries or by further excavation, survey, and sampling of the existing physical remains. In any case such lack of correspondence between historical and archaeological evidence is not at all uncommon in medieval archaeology and does not detract from the value of the complementary radiocarbon dating that this project had made possible.

Acknowledgments

The project took place within the framework of the Leon Levy Expedition to Ashkelon's program of excavation and survey at the site and the collaborative project between the Expedition and Cardiff University focusing on the study of the surviving remains of the Byzantine and medieval town walls (see Chapter 19, this volume). We are particularly grateful to Professor Daniel Master and the Expedition's sponsors for facilitating our work under the auspices of licences granted by the Israel Antiquities Authority. DP was assisted in collecting charcoal samples in July 2012 by Yining Xue (Boston University) and in September 2014 by Hannah Buckingham (Cardiff University), and gratefully acknowledges grants for this and other related work awarded by the Society of Antiquaries of London, the Council for British Research in the Levant, and the Palestine Exploration Fund. The samples were kindly identified by Dr. Stephen Harris of the

Department of Plant Sciences, Oxford University, following which those selected were dated by Professor Tom Higham, Dr. Fiona Brock, and Dr. David Chivall of the Oxford Radiocarbon Accelerator Unit, with funding in all but three cases provided by the United Kingdom's National Environmental Research Council (NERC), to which we are profoundly grateful.